



## Condition Assessment of a Mural Oil Painting at Fatma Ismail Palace, Agricultural Museum, Egypt

Moustafa Attia Mohie<sup>a</sup>, Abubakr Moussa<sup>a</sup>, Rehab Fathey<sup>b</sup>, Shaimaa S. Abdelaziz<sup>a</sup>



<sup>a</sup> Department of Conservation, Faculty of Archaeology, Cairo University, Giza, Egypt.

<sup>b</sup> Department of Conservation, Abu Qir Institute, Alexandria, Egypt.

### Abstract

The present study aims to characterize the components and assess the conditions of a deteriorated mural oil painting at Fatma Ismail Palace (Agricultural Museum), Giza, Egypt. Different analytical techniques were used, i.e., the portable digital optical microscope, stereo microscope, Infrared (IR), Ultraviolet (UV), Scanning Electron Microscopy with EDX (SEM.EDX), X-ray Diffraction (XRD), Fourier Transform Infrared Spectroscopy (FTIR), and Gas Chromatography-Mass Spectrometry (GC MS). The findings illustrated the execution technique and external surface of the mural oil painting. Furthermore, the used microscopes showed various deterioration aspects, including flakes, cleavage, micro-cracks, cracks, as well as detached paint layer and the painting ground from support in some parts. The results of elemental analysis by EDX and XRD showed that the red pigment was red hematite, the yellow pigment was yellow ochre, the blue pigment was ultramarine blue (Lazurite), the green pigment was earth green (Glauconite), and the black pigment was carbon black (Graphite). The analysis of soluble salts showed that NaCl was the most common soluble salt. FTIR analysis determined the medium employed as a binder in the painting ground and plaster layer. It showed the functional group of the plaster layer containing gypsum CaSO<sub>4</sub> · H<sub>2</sub>O without a binder and that of the painting ground consisting of Calcite (CaCO<sub>3</sub>), barite (BaSO<sub>4</sub>), glue, and oil. GC/MS analysis revealed that walnut oil was used as a medium for the pigments. The present paper concluded significant findings about the analytical methods of assessing the conditions and identifying the components of the mural oil painting. It showed that the mural oil painting under study suffered from several deterioration aspects. It recommends that further studies should tackle the conservation steps, i.e., conservation treatment or preventive conservation.

**Keywords:** Mural oil painting; Agricultural Museum; Analytical techniques; Microscopes; Deterioration.

### 1. Introduction

The mural oil painting is defined as a method in which the used oil colors are suspended in a carrier medium of a dry oil [21]. The Egyptians extracted linseed oil from early historical times [15]. Winters [50] mentioned that oil was used as a medium for painting in the 11<sup>th</sup> century. Furthermore, Mayer [21] reported that oil painting was used for decorative purposes in England in the early 13<sup>th</sup> century, continued in the 14<sup>th</sup> century, but was not commonly used until the 15<sup>th</sup> century. It was popularly used by the Flemish artist Jan van Eyck [21, 48, 50]. Then, it moved to Italy by Antonello da Messina [48].

Mural oil paintings are multi-layers [28]. The wall support includes lima stone, red brick, and structural walls [19, 44]. A rough plaster layer consists of sand, gypsum, and lima to give it the required strength, texture, and porousness [6, 5, 26, 28, 42, 16]. The fine plaster layer consists of a mixture of lime and fine sand. It is softer than the previous layer to get a smooth

surface [6, 5]. The painting ground consists of a filling material (white material), such as gypsum, lima, and adhesive material (glue) [14]. Moreover, the paint layer consists of pigment and oil medium (linseed oil, walnut oil, safflower, and poppy seed oil) diluted with plant turpentine or mineral turpentine [48, 43, 45, 50]. Paintings are carried out on the plaster layer, which is applied directly on the wall, on canvas, which covers the wall, or on a panel [31].

Many external and internal factors may cause the deterioration of mural oil paintings. The internal factors result from differences in the physical property among the layers. They result in stress and damage to the mural's original structure when ambient conditions change [14, 18]. They also include the implementation methods and the quality of the materials [5]. In contrast, the external factors are caused by improper environmental circumstances, including relative humidity fluctuation (causing hygric and hydric contraction, weakening, and dissolved binding

\*Corresponding author e-mail: [shimaa-sayed@cu.edu.eg](mailto:shimaa-sayed@cu.edu.eg) (Shaimaa sayed).

Receive Date: 04 August 2022, Revise Date: 24 August 2022, Accept Date: 30 August 2022

DOI: 10.21608/EJCHEM.2022.149749.6472

©2022 National Information and Documentation Center (NIDOC)

medium and other components), temperature fluctuation (causing thermal stress), salts (causing crystal growth stress), excess light, gaseous particulates and pollutants, earthquakes, heavy traffic, and explosion [29, 5, 41, 26, 51, 46, 17, 14, 38, 18, 7, 34, 20, 16].

Several aspects of deterioration are obtainable, e.g., darkening, blanching, fading, craquelure (micro-cracks), cracks [5, 51], flaking of paint layers at many points, detachment from the preparatory and support layers, powdering the mortars [41, 49, 12, 16], salt efflorescence, surface protrusions, plaster detachment [12], and disruption [39, 16].

Researchers utilize several analytical techniques to help identify the components of the studied painting and highlight its deterioration mechanisms to develop a suitable conservation plan. The analytical methods help obtain conservation solutions by defining the extent of deterioration and proposing appropriate conservation methods. Non-destructive techniques (portable equipment) are essential because they play a part in the in situ analyses without sampling. The observation of painting by the portable digital microscope helps the evaluation state of paintings [42]. It was used to examine the external surface, the painting technique of the mural oil painting, and samples containing geomaterials. It also shows the morphology and texture of the parts [2, 23]. A stereo microscope was used to explore the stratigraphy and microscopic features of the paint layers, invisible deterioration, and micro-organism colonies [24, 12]. Infrared (IR) showed the color layers below the surface pigments. Ultraviolet (UV) images revealed anomalies and characteristics of deterioration that are hard to notice [8]. It was used to study the surface and the various deterioration aspects, such as cracks and places of retouching in the previous restoration [23]. Scanning electron microscopy with EDX (SEM.EDX) has high-resolution observation of microstructural characteristics and elemental analysis of the mural paint layers, such as binders and pigments [12]. It utilizes electromagnetic instead of light waves to investigate samples in 3 dimensions. That is, it illustrates a detailed image of the specimen's topography to help investigate the morphology and texture of painting and pigments of the historical samples in high definition and detect their elements in micron-sized areas [43, 2]. X-ray diffraction (XRD) is used to identify the inorganic compounds in the plaster layer, the white material type in the painting ground, and the colored materials [42, 23]. Fourier transform infrared spectroscopy (FTIR) is a non-destructive technique and has been widely used for determining the type of medium used as a bonding material on the painting ground and oil medium [18, 23]. It relies on the absorption of infrared radiation by the material. It helps analyze the various chemical functions of a

molecule via its characteristic vibrations. The compounds were identified by comparing with commercial or laboratory-designed spectral databases [30, 32]. Gas Chromatography mass spectrometry (GC MS) is used to determine the oil medium used in the mural oil painting, which is one of the most important ways to identify the fatty acids that make up the oil medium [15, 18, 23].

The treatment of mural oil painting is a significant process to repair all deterioration forms in the painting. Some conservation treatments are required, including cleaning, consolidation, removing the gypsum stains, treating blanching, treating cracks and micro-cracks, detachment of some parts from mural oil painting and reinstalling them after treatment, reattaching the flaking paint, and retouching.

## 2. Technical study and historical outlines of the case study

The case study of this paper primarily focuses on a unique mural oil painting known in Arabic as "Elsouk Painting", which means "the market painting". It is located in the scientific collection museum at the Egyptian Agricultural Museum in Giza, Egypt [Fig. 1].

King Fuad initiated and executed the idea of the museum foundation (1868-1936) after visiting the Agricultural Museum of Budapest. In the same context, King Fuad issued an official royal decree to the government to establish the museum. It was known then as King Fuad I Agricultural Museum. Due to its uniqueness, the museum was classified as the first of its kind in the Middle East and the second-largest Agricultural Museum worldwide after Budapest.

The palace of Princess Fatima, daughter of Khedive Ismail, in Giza City, was chosen to house the newly established museum, which was officially inaugurated on January 16, 1939 [10].

The painting mainly depicts various vending and buying activities across the market. For instance, the onlooker could observe a seated street vendor and a lady shopper checking the exhibited products.

In 1927, the painting was executed directly on the chosen wall during the actual building activities of the museum.

It consists of a back wall that plays the role of the primary painting support, a rough plaster layer, a fine plaster layer, an underpainting layer (Painting ground), and paint layers. The dimensions of the specified case study part of the mural painting measure 173 cm (long) x 154 cm (wide).



Fig 1. Mural oil painting "El souk Painting"

### 2.1. Documentation of the painting using AutoCAD

Imaged were obtained using AutoCAD that showed Elsouk painting and deterioration aspects, such as blanching, craquelure (micro-cracks), cracks [5, 51], flaking of paint layers at many points [41, 12, 49, 16], disruption [16, 39], cleavage [22], and gypsum stains [Fig. 2].

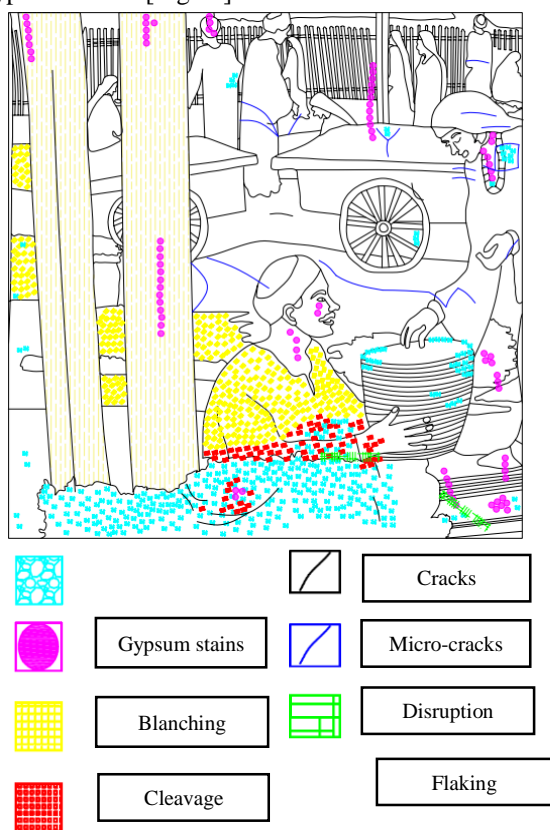


Fig 2. Documentation of the El souk Painting, and deterioration aspects using AutoCAD.

## 3. Materials and methods

### 3.1. Sampling

The researchers collected samples of the plaster layer, painting ground, and small amounts of the red, yellow, blue, green, and black pigments from detached parts of the painting.

### 3.2. Analytical techniques

#### 3.2.1. Portable digital light microscope

The portable digital microscope (1200X is made by ROHS) was used to investigate the surface morphology of the painted layers of the painting. It helped investigate the brushstrokes and identify the pigments mixing method, whether done on the painting or the pallet, using an investigation method known as Vertical Photo Microscope (V.P.M).

#### 3.2.2. Stereo microscope

Stereomicroscope (Leica MZ6) with 80X at the Central Laboratories Sector, the Egyptian Mineral Resources Authority, Ministry of Petroleum was used to study the stratigraphic and microscopic features of the paint layers sample.

#### 3.2.3. Infrared (IR)

IR (PHILIPS, Incandescent 230- 250V BR 125, infrared double reflector system) was used to penetrate below the surface pigments layers and reveal details otherwise difficult to see.

#### 3.2.4. Ultraviolet Examination (UV)

UV (Nikon D90 digital single-lens reflex) was used to study the surface and the various deterioration aspects, such as cracks and places of routing in the previous restoration.

#### 3.2.5. Scanning Electron Microscopy with EDX (SEM.EDX)

SEM.EDX (SEM Model Quanta 250 FEG (Field Emission Gun) attached with EDX Unit (Energy Dispersive X-ray Analyzes), with accelerating voltage 30 K.V., magnification 14x up to 1000000 and resolutions for Gun.1n). FEI Company, the Netherlands) was used at the Central Laboratories Sector, the Egyptian Mineral Resources Authority, Ministry of Petroleum to investigate the surface morphology and texture of the painting and pigments of the historical samples and their elements of micron-sized areas.

#### 3.2.6. X-ray diffraction (XRD)

XRD (device model (Empyrean), step size [ $^{\circ}$ Th.] of 0.0130, scan step time [s] of 29.0700, measurement temperature [ $^{\circ}$ C] of 25.00, anode material of Cu, K-Alpha1 [ $\text{\AA}$ ] of 1.54060, K-Alpha2 [ $\text{\AA}$ ] of 1.54443, K-Beta [ $\text{\AA}$ ] of 1.39225, K-A2 / K-A1 Ratio of 0.50000, and generator settings of 30 mA, 40 kV) was used at the National Institute of Standards to identify the compounds in the plaster layer, the white material type in the ground layer, and the colored materials.

#### 3.2.7. Fourier Transform Infrared Spectroscopy (FTIR)

FTIR with the following specifications (a Nicol 380 spectrophotometer (Thermos Scientific), the

wavenumber range of 4,000-400cm) was used to analyze the sample (0.002g) was mixed with kb to reach (0.2g) to form a round disk suitable for measurement at the National Institute of Standards. It helped determine the type of medium used as a bonding material on the painting ground.

### 3.2.8. Gas Chromatography-Mass Spectrometry (GC/MS)

GC-MS analysis was performed (Agilent Technologies 7890B GC systems combined with 5977A mass selective detector). A capillary column was used (HP-5MS Capillary; 30.0 m × 0.25 mm ID × 0.25 μm film) and the carrier gas was helium at a pressure of 8.2 psi with 1 μl injection. (Jun 2014) at the Faculty of Science, Ain Shams University, to determine the oil medium used in the mural oil painting.

## 4. Results and discussion

### 4.1. Examination of the mural oil painting

#### 4.1.1. Infrared (IR), Ultraviolet (UV)

IR images showed that the pigment layers below the surface pigments didn't appear [Fig. 3 (b)]. UV images revealed the surface and the various deterioration aspects, such as cracks [23] and no previous restoration [Fig. 3 (c)].

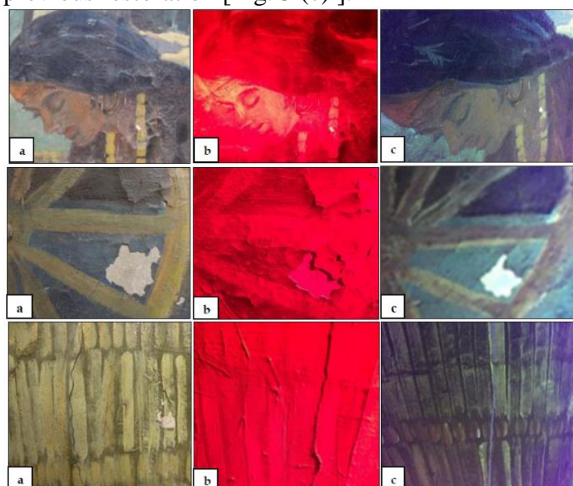


Fig 3. (a) photograph, (b) images under Infrared light, (c) images under Ultraviolet light.

#### 4.1.2. Vertical Photo Microscope (V.P.M)

The images of the V.P.M. illustrated that the artist employed the multi-layer method and fine impasto in some parts of the painted layer and the method of mixing pigments applied directly on the painting [Fig. 4 (a, b, c)].



Fig 4. (a, b, c) showed the multi-layer method and fine impasto in some parts of the painted layer, and the method of mixing pigments applied directly on the painting.

#### 4.1.3. Portable digital light microscope

The optical microscope images illustrated the different deterioration aspects of the mural oil painting, such as cracks [5, 51] [Fig. 5 (a, b)], micro-cracks [43] [Fig. 5 (c, d)], flakes [Fig. 5 (e, f)], cleavage [22] [Fig. 5 (g)], and the detachment of the paint layer and the painting ground from support in some areas [41, 12, 43, 16] [Fig. 5 (h, i)].

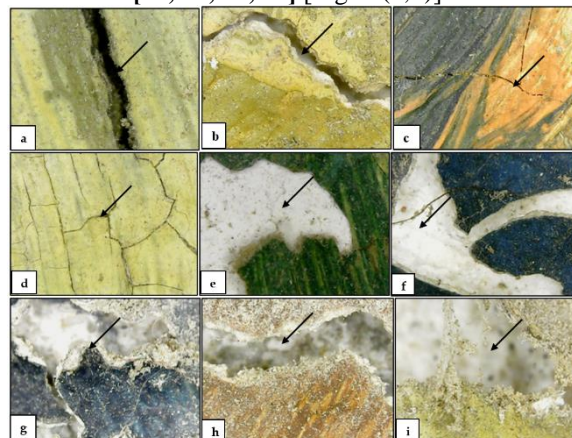


Fig 5. showed the different deterioration aspects of the mural oil painting with the digital light microscope.

Notes: (a, b) cracks, (c,d) micro-cracks, (e, f) flakes, (g) Cleavage, (h, i) detachment of the paint layer and the painting ground from support.

### 4.2. Examination and analysis of the plaster, painting ground, and pigment samples

#### 4.2.1. Plaster layer

The portable digital light microscope images illustrated the fine plaster layer and deterioration aspects, such as micro-cracks, salts, and irregular surfaces [Fig. 6 (a)]. These aspects were also shown by the stereo microscope [Fig. 6 (b)] and SEM. They showed gaps, spaces, unrelated granules, clear surface [Fig. 6 (c)], and the distinctive shape of the gypsum [Fig. 6 (d)]. The EDX analysis illustrated that this layer consisted of Ca (49.57%), S (12.04), O (30.86%), and other elements, as shown in (Table 2). These elements are referred to as gypsum  $\text{CaSO}_4 \cdot \text{H}_2\text{O}$ . To confirm this finding, XRD was applied. It illustrated that the plaster layer sample consisted of gypsum  $\text{CaSO}_4 \cdot \text{H}_2\text{O}$ , which constitutes 93.0%. This result is consistent with Schmidt et al. [42] and Ali et al. [1]. This layer also contained anhydrite (result from around gypsum with high temperature), which constitutes 3.6%, Quartz, which constitutes 1.3%, calcite ( $\text{CaCO}_3$ ), which constitutes 1.1% as a result of the painting ground and the soluble salts extracted from the sample: Halite ( $\text{NaCl}$ ), which constitutes 1.0% [Fig. 6 (e)]. This result is consistent with Bianchin et al. [3]. FTIR spectrum illustrated a functional group of gypsum  $\text{CaSO}_4 \cdot \text{H}_2\text{O}$  due to the stretching band  $\text{SO}_4^{2-}$  at  $1130\text{cm}^{-1}$ , stretching band

S=O at  $1622\text{ cm}^{-1}$ ,  $1686\text{ cm}^{-1}$  and stretching band O-H at  $3404\text{ cm}^{-1}$ ,  $3547\text{ cm}^{-1}$  [Fig. 6 (f)]. This layer consisted of gypsum without a binding material. This finding agrees with Derrick et al. [9] and Salvadori et al. [40].

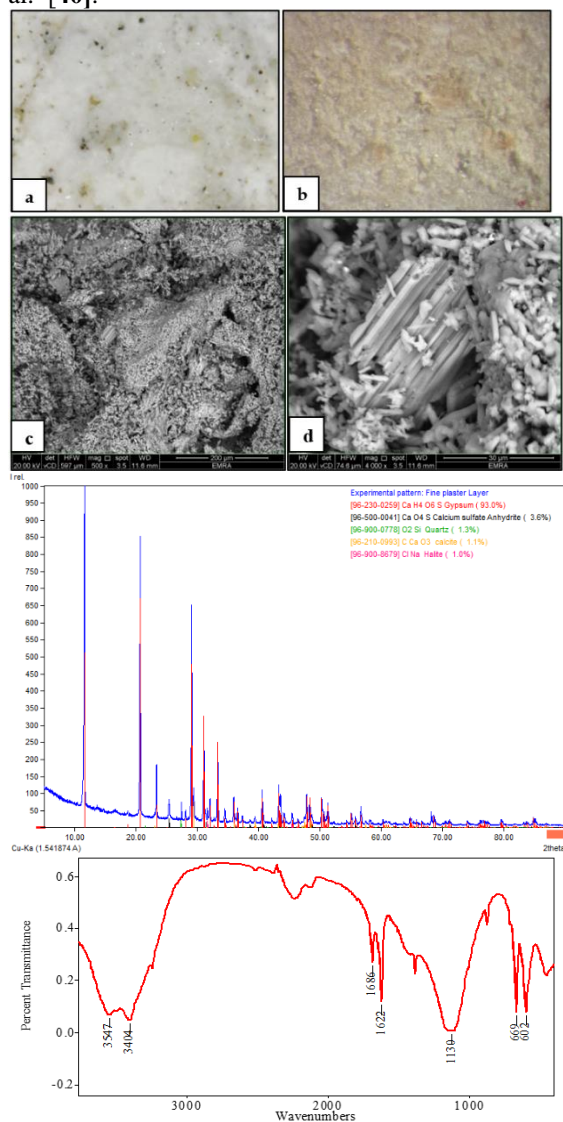


**Fig 6.** Results of examination and analysis of the plaster layer. (a) showed the deterioration aspects of the plaster layer with a digital light microscope X500, (b) showed the deterioration aspects with a stereomicroscope X80. (c) SEM micrographs of the plaster layer, (d) The distinctive shape of the gypsum. (e) XRD chromatogram of the plaster layer. (f) FT-IR spectra of the plaster layer.

#### 4.2.2. painting ground

The images of the portable digital light optical microscope illustrated deterioration aspects, such as salts [Fig. 7 (a)], which were confirmed by the stereo microscope [Fig. 7 (b)] and SEM. They also showed irregular surfaces [Fig. 7 (c)]. SEM also showed micro-cracks, gaps, spaces, unrelated granules, and calcite [Fig. 7 (d)]. The painting ground consisted of a filling material (white material), such as gypsum, lime, and adhesive material (glue) [14]. Analyzing the

painting ground with EDX showed some elements (Table 2), such as C (30.69%), O (41.66%), Ca (11.72%), Ba (3.38%), and others. These elements referred to the use of calcite "calcium carbonate" ( $\text{CaCO}_3$ ) and barite "barium sulfate"  $\text{BaSO}_4$  in the painting ground. To confirm this finding, XRD was applied. It illustrated calcite ( $\text{CaCO}_3$ ) (78.5%), barite ( $\text{BaSO}_4$ ) (8.6%), halite ( $\text{NaCl}$ ) (1.9%), and gypsum  $\text{CaSO}_4 \cdot \text{H}_2\text{O}$  (10.9%) as a result of the plaster layer [Fig. 7 (e)]. FTIR spectrum illustrated the functional groups of calcium carbonate ( $\text{CaCO}_3$ ) with a stretching band  $\text{CO}_3^{2-}$  at  $1419\text{ cm}^{-1}$  and bending band O-C-O at  $874\text{ cm}^{-1}$  and the functional groups of oil with a stretching band O-H at  $3406\text{ cm}^{-1}$  and  $3547\text{ cm}^{-1}$ , stretching band C-H at  $2852\text{ cm}^{-1}$ ,  $2924\text{ cm}^{-1}$ , stretching band C=O at  $1732\text{ cm}^{-1}$ , bending bands C-H at  $1419\text{ cm}^{-1}$ , stretching band C-O at  $1119\text{ cm}^{-1}$ , and torsion band C-H at  $712\text{ cm}^{-1}$ . In addition, it showed the functional groups of glue with a stretching band N-H at  $3248\text{ cm}^{-1}$ , stretching band C-H at  $2852\text{ cm}^{-1}$ ,  $2924\text{ cm}^{-1}$ , stretching band C=O at  $1618\text{ cm}^{-1}$ , bending bands C-N-H at  $1560\text{ cm}^{-1}$ , and bending bands C-H at  $1419\text{ cm}^{-1}$  [Fig. 7 (f)]. This result is consistent with Derrick et al. [9].

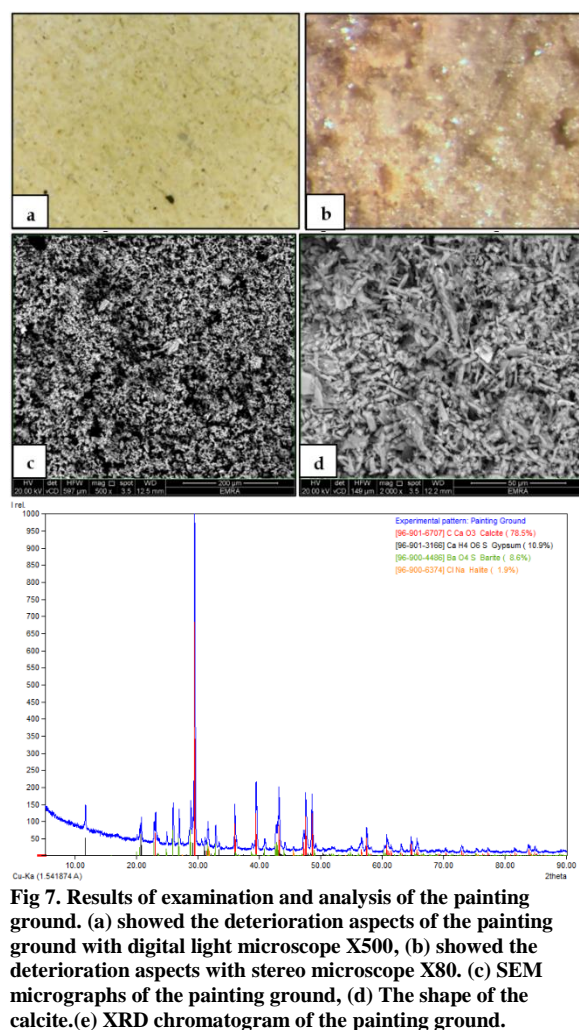
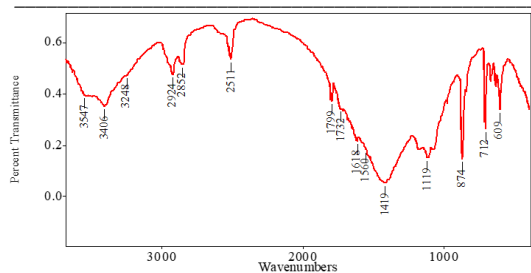


**Fig 7.** Results of examination and analysis of the painting ground. (a) showed the deterioration aspects of the painting ground with digital light microscope X500, (b) showed the deterioration aspects with stereo microscope X80. (c) SEM micrographs of the painting ground, (d) The shape of the calcite. (e) XRD chromatogram of the painting ground.



(f) FT-IR spectra of the painting ground.

### 4.2.3. The Pigments and oil medium

#### 4.2.3.1. The oil medium type

The paint layer consists of pigments and oil media (linseed oil, walnut oil, safflower, and poppy seed oil) diluted with plant turpentine or mineral turpentine [48, 43, 45, 50]. GC MS analysis revealed that the oil medium used was “walnut oil”. Relative amounts of the fatty acids illustrate the drying oils by highlighting the ratios of the peak areas among fatty acids derivatives stearic/palmitic [13, 47]. The analysis results (GC MS) revealed the ratio between the stearic acid [Fig. 8 (a)] (24.54%) and palmitic acid [Fig. 8 (b)] (75.45%) was 0.32, indicating that the oil used was walnut oil (Table 1) [ Fig. 8 (c) ]. This result is consistent with Vicente [47].

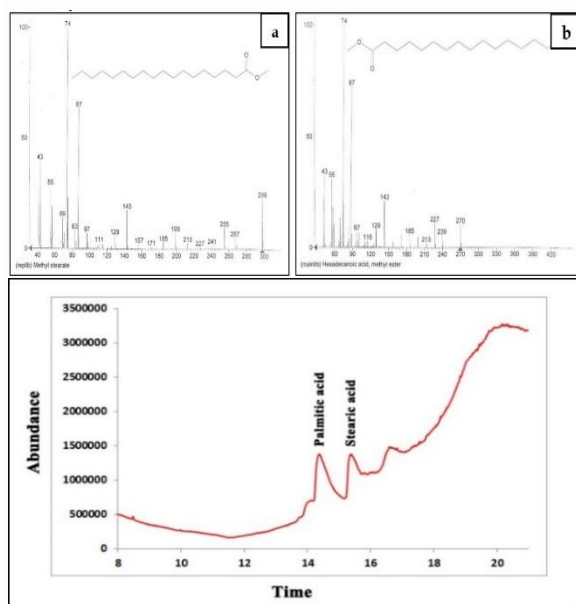


Fig 8. GC – MS analysis results of the oil medium.

(a) GC – MS spectra of the fatty acid (stearic acid), (b) GC – MS spectra of the fatty acid (palmitic acid) in the sample. (c) spectra showed the ratio of the fatty acids (stearic/palmitic) in the sample.

Table 1. showed the ratio of the fatty acids (stearic/palmitic) in the sample.

Fatty Acids	Retention (Min)	Content %
Stearic	15.38	24.54
Palmitic	14.38	75.45

#### 4.2.3.2. The red pigment

Cross-section images of the digital optical microscope illustrated that the artist adopted the multi-layer technique. The artist used a multi-layer for the red pigment with a thickness of 0.02mm [Fig. 9 (a) ]. These images demonstrated deterioration aspects, such as flakes, salts, dust, and dirt [Fig. 9 (b) ]. These aspects appeared with the stereo microscope [Fig. 9 (c) ] and SEM. There were also gaps and spaces, micro-cracks, irregular surfaces, and granules of different sizes [Fig. 9 (d, e) ]. EDX analysis illustrated that the red pigment consisted of O (2.76%), Fe (12.38%), Zn (19.40%), and other elements, as shown in table (Table 2), denoting red hematite. This result is consistent with Bikiaris et al. [4] and Beltran [2]. These elements were mixed with white zinc. To confirm this finding, XRD was applied. XRD analysis illustrated that the red pigment sample consisted of red hematite ( $\text{Fe}_2\text{O}_3$ ), which constitutes (5.3%) [Fig. 9. (f) ]. This result is consistent with Pomies et al. [35], Moussa et al. [26], Gialanella et al. [11], Prieto et al. [36], and Mohie et al. [23]. Hematite was the first pigment of art history [35] . It was obtained by heating goethite up to moderate temperatures (300–350°C), depending on the level of impurities in the material and microstructural features, such as grain size and shape [27]. XRD also showed white zinc (ZnO) (0.9%), as well as calcite and barite because of the painting ground and gypsum as a result of the plaster layer.

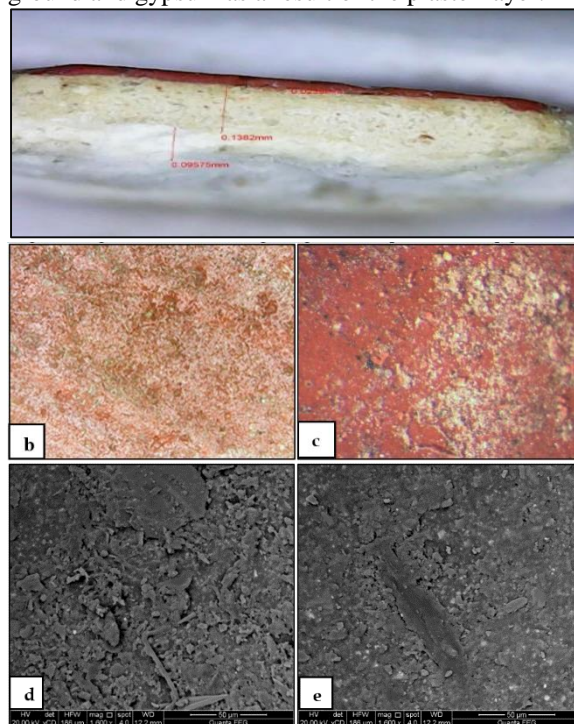
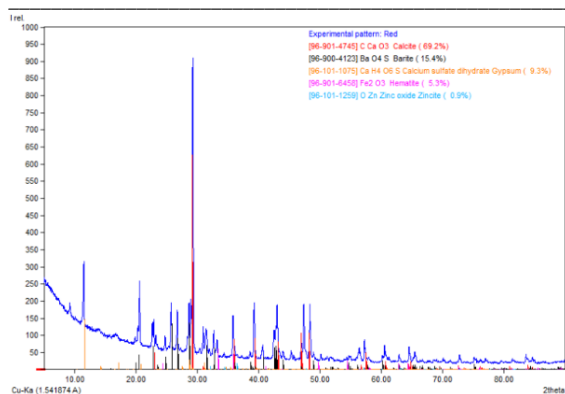


Fig 9. Results of examination and analysis of the red pigment.

(a) showed a cross-section with a digital light microscope X250 for the red pigment sample. (b) showed the deterioration aspects of red pigment with digital light microscope X500, (c) showed the deterioration aspects with stereo microscope X80. (d, e) SEM micrographs for the red pigment.



(f) XRD chromatogram for the red pigment.

#### 4.2.3.3. The yellow pigment

Cross-section images of the digital optical microscope illustrated that the artist adopted the multi-layer technique. The artist used the yellow pigment layer with a thickness of 0.02mm and applied it to several layers of pigments: the red pigment with a thickness of 0.01mm, the white pigment with a thickness of 0.09mm, the black pigment with a thickness of 0.01mm, and the painting ground with a thickness of 0.02mm [Fig. 10 (a) ]. These images showed deterioration aspects, such as irregular surfaces, cracks, dust, salts, and dirt [Fig. 10 (b) ]. These aspects also appeared with the stereo microscope [Fig. 10 (c) ] and SEM. They displayed the shape of granules, micro-cracks, different sizes of granules, gaps, and spaces on the surface [Fig. 10 (d,e) ]. EDX analysis illustrated that the yellow pigment contained O (19.90%), Fe (3.52%), and other elements, as shown in table (Table 2), suggesting the use of yellow ochre  $\text{Fe}_2\text{O}_3 \cdot \text{H}_2\text{O}$  mixed with red hematite ( $\text{Fe}_2\text{O}_3$ ). This result is consistent with Bikiaris et al. [4], Mugnaini et al. [27], Bianchin et al. [3], and Proietti et al. [37]. To confirm it, XRD was applied [Fig. 10 (f) ]. XRD illustrated that the yellow pigment consisted of yellow ochre  $\text{Fe}_2\text{O}_3 \cdot \text{H}_2\text{O}$  (3.3%). This result is consistent with Mugnaini et al. [27] and Prieto et al. [36]. It also contained red hematite (22.2%), as well as calcite and barite as a result of the painting ground.

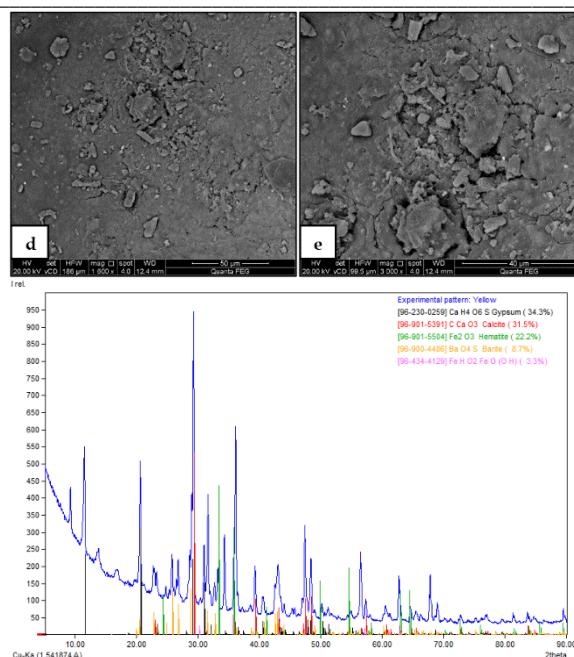
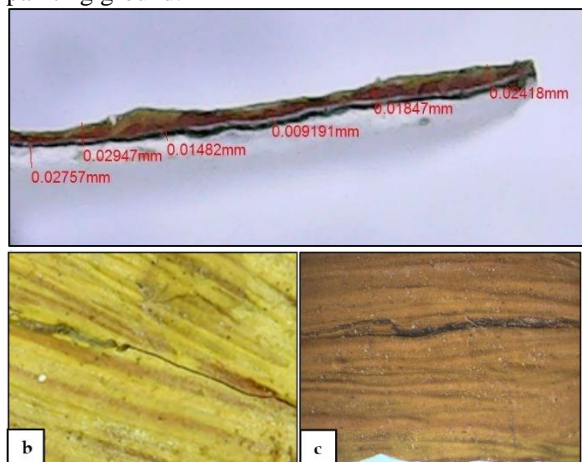
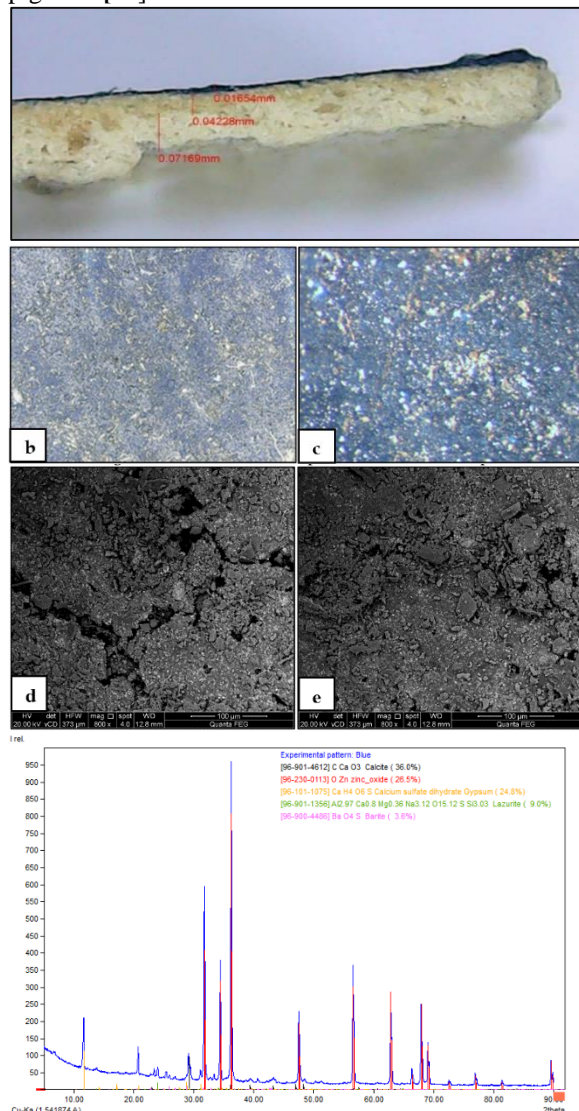


Fig 10. Results of examination and analysis of the yellow pigment. (a) showed a cross-section of digital light microscope X250 for the yellow pigment sample. (b) showed the deterioration aspects of yellow pigment with digital light microscope X500, (c) showed the deterioration aspects with stereo microscope X80. (d, e) SEM micrographs for the yellow pigment. (f) XRD chromatogram for the yellow pigment.

#### 4.2.3.4. The blue pigment

Cross-section images of the digital optical microscope illustrated that the artist adopted the multi-layer technique. The blue pigment layer thickness was 0.01mm [Fig. 11 (a) ]. These images showed deterioration aspects, such as salts, flakes, dust, and dirt surface [Fig. 11 (b) ]. These aspects also appeared with the stereo microscope [Fig. 11 (c) ] and (SEM). Besides, they showed cracks, gaps, spaces, and irregular surfaces [Fig. 11 (d) ], and granules with different sizes [Fig. 11 (e) ]. Analyzing the blue pigment by EDX showed some elements, such as Al (0.73%), Si (0.67), S (6.56) in Spot 1, and Na (2.98%) in Spot 2. These elements referred to the use of ultramarine blue (lazurite) ( $3\text{Na}_2\text{O} \cdot 3\text{Al}_2\text{O}_3 \cdot 6\text{SiO}_2 \cdot 2\text{Na}_2\text{S}$ ). Other elements are shown in (Table 2). To confirm these findings, XRD was applied. XRD analysis showed ultramarine blue (lazurite) (9.0%), white zinc (ZnO) (26.5%), as well as calcite and barite because of the painting ground, and gypsum because of the plaster layer [Fig. 11 (f) ]. The Europeans broadly used the pigment ultramarine in the 14<sup>th</sup> and 15<sup>th</sup> centuries. It was obtained by crushing, grinding, and cleaning the raw material to separate other minerals from lazurite. Using lapis lazuli was limited because it was expensive, and cheaper alternatives were available, including Prussian blue and the potassium-cobalt glass pigment. Nevertheless, in 1828, Jean Baptiste Guimet synthesized ultramarine with a similar chemical

composition to lazurite. Lapis lazuli could be identified by optical microscopy or under SEM because the morphology of its particles and variations in the particle sizes differed from the uniform, small, and round particles of the synthetic ultramarine blue pigment [33].

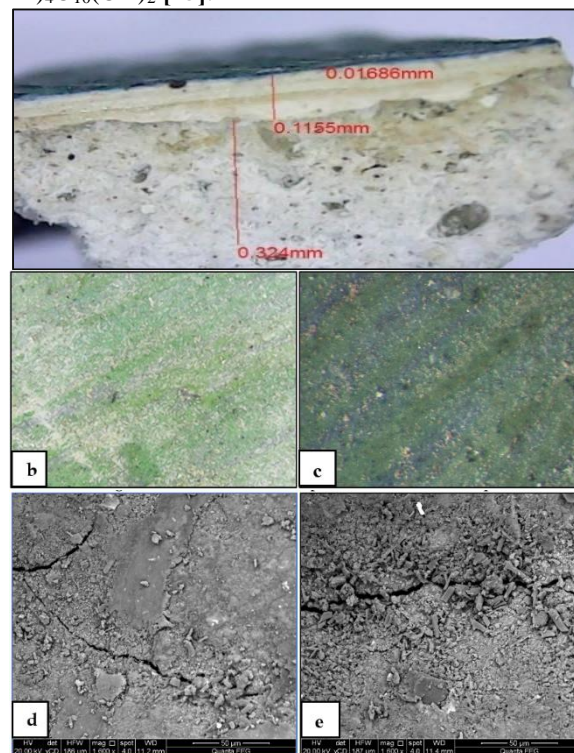


**Fig 11.** Results of examination and analysis of the blue pigment. (a) showed a cross-section of digital light microscope X250 for the blue pigment sample. (b) showed the deterioration aspects of blue pigment with digital light microscope X500, (c) showed the deterioration aspects with stereo microscope X80. (d, e) SEM micrographs for the blue pigment. (f) XRD chromatogram for the blue pigment.

#### 4.2.3.5. The green pigment

Cross-section images of the digital optical microscope demonstrated that the artist employed the multi-layer technique. The green pigment layer consisted of mixed green and blue pigment with a thickness of 0.01mm [Fig. 12 (a)]. It showed the deterioration aspects of the sample, such as salts crystallization on the surface, flakes, dust, and dirt [Fig. 12 (b)]. These aspects also appeared with the

stereo microscope [Fig. 12 (c)] and SEM. They also displayed cracks, gaps, and spaces on the surface, irregular surface, and granules of different sizes [Fig. 12 (e,f)]. EDX analysis showed that the green pigment consisted of Mg (0.20%), Al (0.46%), K (0.28%), and Fe (0.89%), suggesting the use of green earth (Table 2). To confirm this finding, XRD was applied. It illustrated that the green pigment contained earth green (glaucanite), calcite as a result of the painting ground, and gypsum as a result of the plaster layer [Fig. 12 (f)]. The green pigments were copper-based in Egypt, while in the Roman area, the most diffuse green pigments were green earth, mainly celadonite and glaucanite. The green earth was obtained by mixing minerals with different compositions, structures, and colors. The chemical structure of celadonite and glaucanite was complex, with large differences in morphology, crystalline order, and composition. Celadonite had a crystalline structure with a blue nuance, with the following mean chemical formula:  $K(MgFe_2)(Fe_3, Al)[Si_4O_{10}](OH)_2$ . Glaucanite was green earth with a structureless crystalline than celadonite, denoting the main chemical formula  $(K, Na)(Fe_3, Al, Mg)_2(Si, Al)_4O_{10}(OH)_2$  [25].





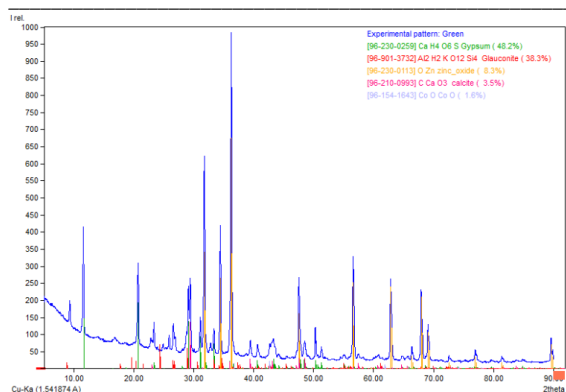


**Fig 12.** Results of examination and analysis of the green pigment. (a) showed a cross-section of digital light microscope X250 for the green pigment sample. (b) showed the deterioration aspects of green pigment with digital light microscope X500, (c) showed the deterioration aspects with stereo microscope X80. (d, e) SEM micrographs for green pigment. (f) XRD chromatogram for the green pigment.

#### 4.2.3.6. The black pigment

The cross-section images by the digital optical microscope illustrated that the artist used the multi-layer technique: The black pigment layer thickness of 0.01mm was applied to several layers of blue pigment with a thickness of 0.02mm [Fig. 13 (a)]. These images showed deterioration aspects, such as salts, flakes, and dust [Fig. 13 (b)] that were highlighted with stereo microscope [Fig 13 (c)], and SEM. In addition, they showed micro-cracks, gaps, spaces, irregular surfaces, and unrelated granules of different sizes [Fig. 13 (d, e)]. According to EDX analysis, the black pigment contained C (49.35%) that was high with other elements, as shown in table (Table 2); this high concentration referred to the use of carbon black “graphite” (C). This result is consistent with Beltran [2] and Proietti et al. [37]. To confirm this finding, XRD was applied. It showed that the black pigment contained carbon black “graphite” (C), calcium carbonate as a result of the painting ground, and gypsum as a result of the plaster layer [Fig. 13 (f)].

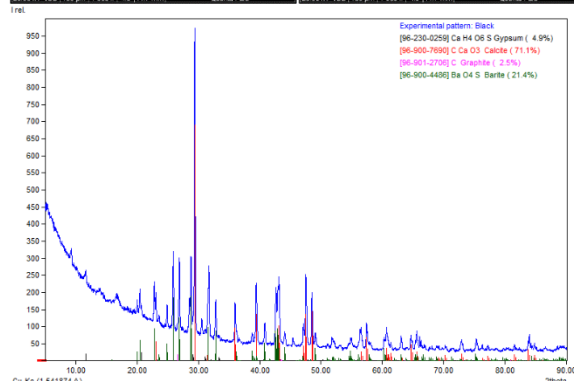
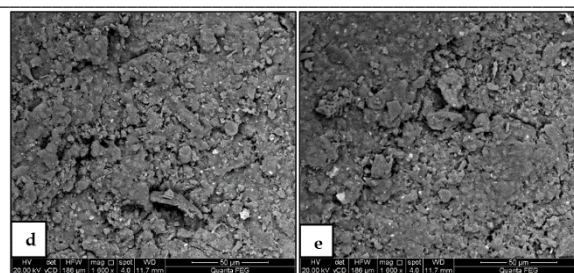
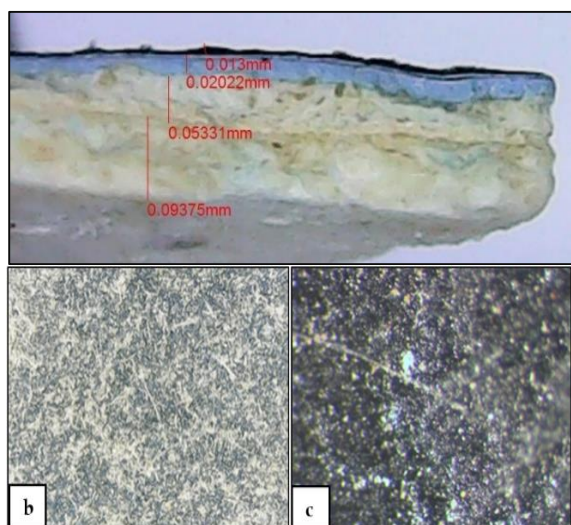


**Fig 13.** Results of examination and analysis of the black pigment. (a) showed a cross-section of digital light microscope X250 for black pigment sample. (b) showed the deterioration aspects of black pigment with digital light microscope X500, (c) showed the deterioration aspects with stereo microscope X80. (d, e) SEM micrographs for the black pigment. (f) XRD chromatogram for the black pigment.

**Table 2.** EDX analysis results of the plaster, painting ground, and pigment samples.

Elements	plaster layer (Mass%)	Painting ground (Mass%)	Red pigment (Mass %)	Yellow pigment (Mass %)	Blue pigment Spot 1 (Mass %)	Blue pigment Spot 2 (Mass %)	Green pigment (Mass %)	Black pigment (Mass %)
C	6.00	30.69	2.43	16.96	51.87	56.21	8.51	49.35
O	30.86	41.66	2.76	19.90	19.60	14.60	9.79	16.80
Na	0.00	4.49	0.00	0.00	0.00	2.98	0.00	2.93
Al	0.00	0.00	0.77	0.89	0.73	0.74	0.46	0.56
Mg	0.00	1.50	0.00	0.00	0.00	0.00	0.20	0.00
Si	1.53	1.94	0.00	1.02	0.67	0.60	0.76	0.40
S	12.04	4.00	4.19	13.36	6.56	6.60	4.93	3.60
Cl	0.00	0.62	0.61	1.58	0.00	0.00	1.64	2.36
Ag	0.00	0.00	0.00	1.12	0.00	0.00	0.00	0.00
Ca	49.57	11.72	18.73	16.64	15.07	8.36	7.53	16.71
Cs	0.00	0.00	2.36	0.00	0.00	0.00	0.00	0.00
Ba	0.00	3.38	24.67	19.03	0.00	0.00	2.74	7.29
Ce	0.00	0.00	5.91	0.00	0.00	0.00	0.64	0.00
Eu	0.00	0.00	5.77	0.00	0.00	0.00	0.00	0.00
Fe	0.00	0.00	12.38	3.52	0.00	0.00	0.89	0.00
Zn	0.00	0.00	19.40	6.25	4.93	0.00	61.63	0.00
Sn	0.00	0.00	0.00	0.00	0.56	0.00	0.00	0.00
Mo	0.00	0.00	0.00	0.00	0.00	7.51	0.00	0.00
K	0.00	0.00	0.00	0.00	0.00	0.00	0.28	0.00

## 5. Conclusions

Microscopic investigations illustrated using a multi-layer method and fine impasto in some parts of the painted layer. The artist did color mixing directly on the artwork. The investigations also showed some deterioration aspects, such as cracks, micro-cracks, flakes, salts, cleavage, and the detachment of the paint layer and the painting ground from support in some parts of the mural oil painting. Infrared (IR) revealed pigment layers below the surface pigments layers, and Ultraviolet (UV) revealed the surface and the various deterioration aspects mentioned above. The analysis

results by (GC MS) showed that the color medium used was walnut oil. The results of elemental analysis by EDX revealed the presence of the main elements of gypsum, including Ca, S, and O in the fine plaster layer and the main elements of calcite and barite, such as C, O, Ca, and Ba in the painting ground. The red pigment was characterized by O, Fe, and Zn correlated with red hematite mixed with zinc white. Analyzing the yellow pigment by EDX illustrated some elements, such as O and Fe. These elements referred to the use of yellow ochre. The blue pigment elements, such as Al, Si, S, and Na, indicated ultramarine blue (Lazurite). The identified elements from the green pigment by EDX analysis were Mg, Al, K, and Fe, referred to as green earth. Analyzing the black pigment by EDX illustrated that C was high, suggesting the use of carbon black "graphite". The FTIR analysis showed that gypsum was used as a filler and binder material for the fine plaster layer. Additionally, the artist used glue for the painting ground.

The study findings attained with the help of several methods of analyses and examinations illustrated that the mural oil painting had many deterioration manifestations. Thus, urgent conservation actions should be carried out, including cleaning, consolidating, removing gypsum stains, treating blanching, and handling microcracks and cracks. They also include attaching the attached parts, reinstalling after handling, reattaching the flaking paint, and retouching.

## References

1. Ali, M. F., Moussa, A., El-sayed, S. H. (2022). Analytical Physicochemical Survey of The Recently Excavated Murals at The Tomp of Iwrakhy/Hatla at Saqqara, Egypt, *Scientific Culture*, Vol. 8, pp. 63-79. DOI: 10.5281/zenodo.571716
2. Beltran, M. P., Submerged villages. recovering wall paintings from the church of Atance (Guadalajara, Spain). Technical study, Exhibition, and 3D display. *International Journal of Conservation Science*, Vol. 7, (2016), pp.1031-1046.
3. Bianchin, S., Casellato, U., Favaro, M. and Vigato, P. A., Painting technique and state of conservation of wall paintings at Qusayr Amra, Amman- Jordan, *Journal of Cultural Heritage*, Vol. 8, (2007), pp. 289-293. DOI: 10.1016/j.culher.2007.05.002
4. Bikiaris, D., Daniilia, S., Sotiropoulou, S., Katsimbiri, O., Pavlidou, E., Moutsatsou, A.P. and Chrysoulakis, Y., Ochre-differentiation through micro-Raman and micro-FTIR spectroscopies: application on wall paintings at Meteora and Mount Athos, Greece. *Spectrochimica Acta Part A*, Vol. 56, (1999), PP. 3-18. DOI: 10.1016/s1386-1425(99)00134-1
5. Calicchia, P. and Cannelli, G. B., Detecting and mapping detachments in mural paintings by non-invasive acoustic technique: measurements in antique sites in Rome and Florence. *Journal of Cultural Heritage*, Vol. 62), (2005), PP. 115: 124. DOI: 10.1016/j.culher.2004.11.001
6. Castellano, A., Cesareo, R., Buccolieri, G., Donativi, M., Palama, F., Quarta, S., De Nunzio, G., Brunetti, A., Marabelli, M. and Santamaria, U., Detection of detachments and inhomogeneities in frescos by Compton scattering, *Nuclear Instruments and Methods in Physics Research B*, vol. 234, (2005), pp. 548:554. DOI: 10.1016/j.nimb.2005.02.012
7. Catalano, J., Murphy, A., Yao, Y., Zumbulyadis, N., Centeno. S.A. and Dybowski, C., Molecular dynamics of palmitic acid and lead palmitate in cross-linked linseed oil films: Implications from deuterium magnetic resonance for lead soap formation in traditional oil paintings. *Solid State Nuclear Magnetic Resonance*, (2017), pp.1-6. DOI: 10.1016/j.ssnmr.2017.12.003
8. Del Lama, E. A., Tirello. R.A., De Andrade, F. R. D. and Kihara, Y., Study of mural paintings by Fulvio Pennacchi in São Paulo City. *Anais da Academia Brasileira de Ciências*, Vol. 81, (2009), pp. 115-126. DOI: 10.1590/s0001-37652009000100012
9. Derrick, M. R., Stulik, D., and Landry, J. M., *Infrared Spectroscopy in Conservation Science*. The Getty Conservation Institute, Los Angeles, (1999), p. 181, 185, 194.
10. Fouad. H.A., Art Collections at Princess Fatima Ismail Palace at the Agricultural Museum in Dokki. Master's Degree, Islamic Department, Faculty of Archaeology, Cairo University, (2021), p. 21-22.
11. Gialanella, S., Belli, R., Dalmeri, G., Lonardelli, I., Mattarelli, M., Montagna, M. and Toniutti, L., Artificial or natural origin of Hematite-Based red pigments in Archaeological contexts: The case of Riparo Dalmeri (Trento, Italy). *Archaeometry*, Vol. 53, (2011), pp. 950-962. DOI: 10.1111/j.1475-4754.2011.00594.x
12. Gil, M., Martins, M. R., Carvalho, M. L., Souto, C., Longelin, S., Cardoso, A., Mirão, J. and Candeias, A. E., Microscopy and Microanalysis of an extreme case of salt and biodegradation in 17th century wall paintings, *Microscopy and Microanalysis*, vol. 21, (2015), pp. 606-616. DOI: 10.1017/s1431927615000562
13. Gimeno-Adelantado, J.V., Mateo-Castro, R., Domenech-Carbo, M.T., Bosch-Reig, F., Domeenech-Carbo, A., Casas-Catalan, M. J. and Osete-Cortina, L., Identification of lipid binders in paintings by gas chromatography: Influence of the pigments. *Journal of Chromatography A*, Vol. 922,

- (2001), pp. 385–390. DOI: 10.1016/s0021-9673(01)00914-1
14. He, X., Xu, M., Zhang, H., Zhang, B. and Su, B., An exploratory study of the deterioration mechanism of ancient wall paintings based on thermal and moisture expansion property analysis, *Journal of Archaeological Science*, Vol. 42, (2014), pp.194:200. DOI: 10.1016/j.jas.2013.10.035
  15. Izzo, F. C., Ferriani, B., Berg, K.J.V.D, Keulen, H.V. and Zendri, E., 20th century artists' oil paints: The case of the Olii by Lucio Fontana. *Journal of Cultural Heritage*, vol.15, (2014), pp. 557-563. DOI:10.1016/j.culher.2013.11.003
  16. Jia, Q., Chen, W., Tong, Y. and Guo, Q., Experimental study on capillary migration of water and salt in wall painting Plaster: A case study at Mogao Grottoes, China, *International Journal of Architectural Heritage*, (2020), pp.1- 12. DOI:10.1080/15583058.2020.1839598
  17. Kamh, G. M. E., Shehata, A. A., Oguchi, C. T., Rabea, R. A. and El-Sayed, S. S. M., Geological and Geotechnical parameters controlling wall paints detachment at selected XXVI dynasty tombs, Bahariya Oasis, Egypt. *Restoration of Buildings and Monuments*, vol. 19, (2013), pp. 11-30. DOI: 10.1515/rbm-2013-6570
  18. Kehlet, C., Kuvvetli, F., Catalano, A. and Dittmer, J., Solid-state NMR for the study of Asger Jorn's paintings. *Microchemical Journal*, vol. 125, (2015), pp. 308- 314. DOI: 10.1016/j.microc.2015.11.010
  19. Lepot, L., Denoel, S. and Gilbert, B., The technique of the mural paintings of the Tournai Cathedral. *Journal of Raman Spectroscopy*, vol.37, (2006), pp.1098-1103. DOI: 10.1002/jrs.1578
  20. Liu, H., Wang, X., Guo, Q., Zhang, M., and Wang, Y., Experimental investigation on the correlation between rainfall infiltration and the deterioration of wall paintings at Mogao, Grottoes, China. *Bulletin of Engineering Geology and the Environment*, Vol. 11, (2019), DOI: 10.1007/s10064-019-01645-5
  21. Mayer, R., *The Artist's Handbook of Materials and Techniques*, 3rd editions Revised and Expanded. New York, USA, The Viking Press, (1978), p. 123, 126.
  22. Mohie, M.A., Scientific approach to the study of the restoration and conservation of oil paintings, Egypt, (2020), p. 50.
  23. Mohie, M. A., Ali, N. M. and Bani Issa, A. A., A new method of lining oil paintings using polyurethane, *Mediterranean Archaeology and Archaeometry*, Vol. 19, (2019), pp. 9-21. DOI: 10.5281/zenodo.3066004
  24. Mohie, M.A., and Sultan, G.M., Analytical study and structural treatment for a thin panel painting, *Pigment and Resin Technology*, Vol. 50, (2021), pp. 104-112.
  25. Moretto, L.M., Orsega, E.F. and Mazzocchin, G.A., Spectroscopic methods for the analysis of celadonite and glauconite in Roman green wall paintings, *Journal of Cultural Heritage*, vol. 12, (2011), pp.384–391. DOI: 10.1016/j.culher.2011.04.003
  26. Moussa, A. M. A, Kantiranis, N., Voudouris, K. S., Stratis, J. A., Ali, M. F. and Christaras, V., The impact of soluble salts on the deterioration of pharaonic and Coptic wall painting at Qurna, Egypt: Mineralogy and chemistry, *Archaeometry*, vol. 51, (2009), pp. 292–308. DOI: 10.1111/j.1475-4754.2008.00422.x
  27. Mugnaini, S., Bagnoli, A, Bensi, P., Droghini, F., Scala, A. and Guasparri, G., Thirteenth century wall painting under the Seine Cathedral (Italy). Mineralogical and Petrographic study of materials, painting techniques, and state of conservation, *Journal of Cultural Heritage*, Vol. 7, (2006), pp. 171-185. DOI: 10.1016/j.culher.2006.04.002
  28. Negur, J. and Alef, Y., Excavation and Treatment of Plaster, Stucco and Wall Paintings in Archaeological Sites, The Israel Antiquities Authority, (2014), p.6.
  29. Nisbeth, A., Deterioration and restoration of some Swedish mural paintings. *Studies in Conservation*, Vol. 25, (1980), pp. 126-129. DOI: 10.1179/sic.1980.25.supplement-1.126
  30. Normand, L., Duchene, S., Verges-Belmin, V., Dandrelc, C., Giovannacci, D. and Nowik, W., Comparative in Situ Study of Nanolime, Ethyl Silicate, and Acrylic Resin for Consolidation of Wall Paintings with High Water and Salt Contents at the Chapter Hall of Chartres Cathedral. *International Journal of Architectural Heritage*, (2020), pp.1-14. DOI: 10.1080/15583058.2020.1731628
  31. NourEdeen. Z.M., Wall painting in Alexandria from the beginning of the 19th century to the mid-20th century, Maser's, Faculty of Fine Arts, University of Alexandria, (2001), P.100.
  32. Nunes, C., Macova, P., Frankeova, D., Sevcik, R. and Viani, A., Influence of linseed oil on the microstructure and composition of lime and lime-metakaolin pastes after a long curing time. *Construction and Building Materials*, Vol. 189, (2018), pp.787-796. DOI: 10.1016/j.conbuildmat.2018.09.054
  33. Osticioli, L., Mendes, N.F.C., Nevin, A., Gil, F.P.S.C., Becucci, M. and Castellucci, E., Analysis of natural and artificial ultramarine blue pigments using laser induced breakdown and pulsed Raman spectroscopy, statistical analysis and light microscopy, *Spectrochimica Acta Part A: Molecular and Biomolecular Spectroscopy*, Vol. 73, (2009), pp. 525–531, DOI: 10.1016/j.saa.2008.11.028

34. Pereira-Pardo, L., Prieto, B., and Silva, B., Assessing the risk of salt decay for wall painting in historic building. thermo-dynamic modeling and transition cycles count. *International Journal of Conservation Science*, Vol. 8, (2017), pp. 351-364.
35. Pomies, M. P. and Menu, M., Vignaud, C., Red palaeolithic pigments: natural Hematite or heated Goethite, *Archaeometry*, Vol. 41, (1999), pp. 275-285. DOI: 10.1111/j.1475-4754.1999.tb00983.x
36. Prieto, G., Wright, V., Burger, R. L., Cooke, C. A., Zeballos-Velasquez, E. L., Watanave, A., Suchomel, M.R. and Suescun, L., The source, processing, and use of red pigment based on hematite and cinnabar at Gramalote, an early Initial Period (1500–1200 cal. B.C.) maritime community, north coast of Peru. *Journal of Archaeological Science*, (2016), pp.45–60.
37. Proietti, N., Tullio, V. D., Presciutti, F., Gentile, G., Brunetti, B. G. and Capitani, D., A multi-analytical study of ancient Nubian detached mural paintings. *Microchemical Journal*, vol. 124, (2016), pp. 719-725. DOI: 10.1016/j.microc.2015.10.022
38. Rosado, T., Mirao, J., Candeias, A., and Caldeira, A.T., Mural paintings deterioration – a multianalytical approach. *Microscopy Society of America*, Vol. 21, (2015), pp. 152-153. DOI: 10.1017/s1431927614014469
39. Saladino, M., Ridolfi, S., Carocci, I., Martino, D., Lombardo, R., Spinella, A., Traina, G. and Caponetti, E., A multi-analytical non-invasive and micro-invasive approach to canvas oil paintings. General considerations from a specific case. *Microchemical Journal*, Vol. 133, (2017), pp.607-613. DOI: 10.1016/j.microc.2017.04.039
40. Salvadori, B., Errico, V., Mauro, M., Melnik, E. and Dei, L., Evaluation of Gypsum and Calcium Oxalates in Deteriorated Mural Paintings by Quantitative FTIR Spectroscopy, *Spectroscopy Letters*, Vol. 36, (2003), pp. 501–513. DOI: 10.1081/sl-120026615
41. Sawdy, A. and Heritage, A., Evaluating the influence of mixture composition on the kinetics of salt damage in wall paintings using time lapse video imaging with direct data annotation. *Environmental Geology*, Vol. 52, (2007), pp. 303-315. DOI: 10.1007/s00254-006-0496-6
42. Schmidt, B. A., Ziemann, M. A., Pentzien, S., Gabsch, T., Koch, W. and Kruger, J., Technical analysis of a Central Asian wall painting detached from a Buddhist cave temple on the northern silk road, *Studies in Conservation*, (2015), pp. 1: 10. DOI:10.1179/2047058414Y.0000000152
43. Serifaki, K., Boka, H., Yalcin, S. and Ipekoglu, B., Characterization of materials used in the execution of historic oil paintings by XRD, SEM-EDS, TGA, and LIBS analysis. *Materials Characterization*, vol. 60, (2009), pp. 303 – 311. DOI: 10.1016/j.matchar.2008.09.016
44. Sheweka, S., Using Mud Bricks as a Temporary Solution for Gaza Reconstruction. *Energy Procedia*, vol. 6, (2011), pp. 236-240. DOI: 10.1016/j.egypro.2011.05.027
45. Speed, H., *Oil Painting Techniques and Materials*. New York: INC. (2012), p.73.
46. Tullio, V., Proietti, N., Gobbino, M., Capitani, D., Olmi, R., Priori, S., Riminesi, C. and Giani, E., Non-destructive mapping of dampness and salts in degraded wall paintings in hypogeous buildings: the case of St. Clement at mass fresco in St. Clement Basilica, Roma. *Anal Bioanal Chem*, (2010), pp.1885-1896. DOI: 10.1007/s00216-009-3400-x
47. Vicente, J.P., Adelantado, J.V.G., Carbo, M.T.D., Castro, R.M. and Reig, F.B., Identification of drying oils used in pictorial works of art by liquid chromatography of the 2-nitrophenylhydrazides derivatives of fatty acids. *Talanta*, Vol. 64, (2004), pp. 326–333. DOI: 10.1016/j.talanta.2004.02.035
48. Viguierie, L., Ducouret, G., Lequeux, F., Moutard-Martin, T. and Walter, P., Historical evolution of oil painting media: A rheological study. *Comptes Rendus Physique*, vol. 10, (2009), pp.612–621. DOI: 10.1016/j.crhy.2009.08.006
49. Vizarova, K., Rehakova, M., Kirschnerova, S., Peller, A., Simon, P. and Mikulasik, R., Stability studies of materials applied in the restoration of a baroque oil painting. *Journal of Cultural Heritage*, vol. 12, (2011), pp.190 -195. DOI: 10.1016/j.culher.2011.01.001
50. Winters, V., *Creative Techniques in Colored Pencil, Graphite, and Oil Painting: Step-by-Step Projects for Teens and Adults*. United States, (2013), pp.18. 20.
51. Zehnder, K. and Voute, A., Monitoring detaching murals in the convent of Müstair (Switzerland) by mirror micrometry, *Journal of Cultural Heritage*, Vol. 10, (2009), pp. 493-500. DOI: 10.1016/j.culher.2009.03.002